In Situ Solid-State NMR Studies of Trichloroethylene Photocatalysis: Formation and Characterization of Surface-Bound Intermediates

Son-Jong Hwang, Chris Petucci, and Daniel Raftery*

Contribution from the Department of Chemistry, H. C. Brown Laboratory, Purdue University, West Lafayette, Indiana 47907-1393

Received December 10, 1997

Abstract: *In situ* solid-state NMR methodologies have been employed to investigate the photocatalytic oxidation of trichloroethylene (TCE) over two TiO_2-based catalysts, Degussa P-25 powder and a monolayer TiO_2 catalyst dispersed on porous Vycor glass. ^{13}C magic angle spinning (MAS) experiments reveal that similar reaction intermediates form on the surfaces of both catalysts. Long-lived intermediates, including dichloroacetyl chloride ($Cl_2HCCOCl$, DCAC), carbon monoxide, and pentachloroethane and final products CO_2, phosgene (Cl_2CO), and HCl were observed under dry conditions. The presence of molecular oxygen was found to be essential for TCE photooxidation to proceed. Adsorbed water was found to greatly reduce the formation of phosgene. The formation of surface-bound dichloroacetate and trichloroacetate species was observed and identified via ^{13}C cross polarization MAS experiments. Dichloroacetate, which forms from mobile DCAC, appears to be bound to the nonirradiated surfaces of the powdered TiO_2 catalyst and further degradation was not possible. Formation of di- and trichloroacetate also takes place on the TiO_2/PVG catalyst in the absence of light; however, their concentrations are low. Degradation studies of these surface-bound species indicate that the photooxidation of dichloroacetate is slow and results in the formation of phosgene and CO_2, while trichloroacetate remains resistive to degradation on the TiO_2/PVG catalyst. Our results also indicate that the formation of DCAC and phosgene seems to be a general result of TCE degradation which is not limited to TiO_2 photocatalysis but instead may be more characteristic of the types of initiating species which are formed by UV irradiation. However, the TiO_2 surface is the most effective in terms of the observed initial rates of degradation.

I. Introduction

Heterogeneous semiconductor photocatalysis represents an emerging area of environmental catalysis with the broadly defined goal of efficiently detoxifying hazardous organic pollutants. Photocatalytic processes using a variety of semiconductor materials has been intensively investigated after an initial report that indicated the potential of TiO_2 materials for photochemical conversion and light harvesting.[1] Presently, a growing interest has developed for efficient and inexpensive methodologies to reduce environmental problems caused by toxic chemicals.[2,3] Due to its stability and nontoxicity, TiO_2 has been most frequently investigated for the degradation of a variety of environmentally harmful organic molecules including halogenated and nonhalogenated compounds. A number of researchers have reviewed the important features of TiO_2 surface chemistry at both the liquid−surface and gas−surface interfaces.[4−7]

There has been a great deal of interest in the photooxidation of trichloroethylene (TCE) due to its role as a significant environmental contaminant. Chlorine photosensitized oxygen inhibition and $O(^3P)$ initiated oxidation of TCE with molecular oxygen were established two decades ago.[8−10] More recently, studies of the photocatalytic oxidation of TCE using semiconductor photocatalysts have been reported at both the liquid−solid[11−17] and gas−solid[16−36] interfaces. Currently, the variety

(1) Fujishima, A.; Honda, K. *Nature* **1972**, *37*, 238.
(2) Schiavello, M. In *Photocatalysis and Environment: Trends and Applications*; Schiavello, M., Ed.; NATO ASI Series C; Boston, 1987; Vol. 237, p 351.
(3) Mills, A.; Davies, R. H.; Worsley, D. *Chem. Soc. Rev.* **1993**, *22*, 417.
(4) Fox, M. A.; Dulay, M. T. *Chem. Rev.* **1993**, *93*, 341.
(5) Hoffmann, M. R.; Martin, S. T.; Choi, W.; Bahnemann, D. W. *Chem. Rev.* **1995**, *95*, 69.
(6) Linsebigler, A. L.; Lu, G.; Yates, J. T., Jr. *Chem. Rev.* **1995**, *95*, 735.
(7) Hagfeldt, A.; Gratzel, M. *Chem. Rev.* **1995**, *95*, 49.
(8) Bertrand, L.; Franklin, J. A.; Goldfinger, P.; Huybrechts, G. *J. Phys. Chem.* **1968**, *72*, 396.
(9) Sanhueza, E.; Hisatsune, I. C.; Heicklen, J. *Chem. Rev.* **1976**, *76*, 801.
(10) Sanhueza, E.; Heicklen, J. *Int. J. Chem. Kinetics* **1974**, *6*, 553.
(11) Pruden, A. L.; Ollis, D. F. *J. Catal.* **1983**, *82*, 404.
(12) Ahmed, S.; Ollis, D. F. *Solar Energy* **1984**, *32*, 597.
(13) Zhang, Y.; Crittenden, J. C.; Hand, D. W.; Perram, D. L. *Environ. Sci. Technol.* **1994**, *28*, 435.
(14) Glaze, W. H.; Kenneke, J. F.; Ferry, J. L. *Environ. Sci. Technol.* **1993**, *27*, 177.
(15) Matthews, R. W. *J. Catal.* **1988**, *111*, 264.
(16) Lichtin, N, N.; Avudaithai, M. *Environ. Sci. Technol.* **1996**, *30*, 2014.
(17) Larson, S. A.; Falconer, J. L. In *Photocatalytic Purification and Treatment of Water and Air*; Ollis, D. F., Al-Ekabi, H., Eds.; Elsevier: Amsterdam, 1993; p 473.
(18) Hwang, S. -J.; Petucci, C.; Raftery, D. *J. Am. Chem. Soc.* **1997**, *119*, 7877.
(19) Fan, J.; Yates, Jr. J. T. *J. Am. Chem. Soc.* **1996**, *118*, 4686.
(20) Hung, C.-H.; Marinas, B. J. *Environ. Sci. Technol.* **1997**, *31*, 562.
(21) Hung, C.-H.; Marinas, B. J. *Environ. Sci. Technol.* **1997**, *31*, 1440.
(22) Nimlos, M. R.; Jacoby, W. A.; Blake, D. M.; Milne, T. A. *Environ. Sci. Technol.* **1993**, *27*, 732.
(23) Jacoby, W. A.; Nimlos, M. R.; Blake, D. M.; Noble, R. D.; Koval, C. A. *Environ. Sci. Technol.* **1994**, *28*, 1661.
(24) Larson, S. A.; Falconer, J. L. *Appl. Catal. B: Environ.* **1994**, *4*, 325.
(25) Berman, E.; Dong, J. In *Chemical Oxidation: Technologies for the Ninties*; Eckenfelder, W. W., Bowers, A. R., Roth, J. A., Eds.; Technomic Pub. Co., Inc.: Lancaster, 1993; p 183.

S0002-7863(97)04192-9 CCC: $15.00
Published on Web 04/23/1998

of different approaches to TCE detoxification is growing and includes the oxidation by nanoscale iron particles[37] and biotransformation methods.[38−41] In the present work, the photocatalytic oxidation of TCE on TiO_2 catalysts was investigated with an aim of examining surface reaction mechanisms.

The photocatalytic activity of TiO_2 is known to result from the generation of electron-hole pairs in the bulk semiconductor which can migrate to the surface and form OH and O_2^- radicals. Both of these radical species have the potential to oxidize organic molecules at the TiO_2 surface. However, despite the contributions from a number of research groups, detailed mechanisms of the photocatalytic oxidation processes at the TiO_2 surface remain elusive, particularly regarding the initial steps involved in the radical reactions, which may involve one or more of the following radical species: O_2^-, OH, and Cl. Although complete mineralization may occur, the reaction mechanisms are complex as demonstrated by the large number of intermediates that have been observed. This situation is particularly evident in reaction conditions where the oxygen concentration is low.[20,21] Regarding mechanisms, the relative roles of O_2^-, OH and Cl as initiating species are still under consideration. Identification of dichloroacetaldehyde (Cl_2-CHCHO) as an intermediate led to the postulation that OH radicals acted as the initiating oxidizing agent.[11,42] In this scenario, the role of molecular oxygen on the TiO_2 surface was limited to electron-trapping. Based on the same intermediate, a reductive pathway[14] involving either the direct capture of a photoexited electron by TCE and/or possible initiation by hydroperoxyl radical (HOO)[30] was also suggested. On the other hand, identification of dichloroacetyl chloride ($Cl_2CHCOCl$, DCAC) as a major intermediate in studies by Nimlos and coworkers at the gas−solid interface[22] as well as the observed high quantum yield (molecules degraded/incident photon) invoked the reconsideration of previous work on chlorine photosensitized oxygen inhibition[8−10] and resulted in the adoption of a Cl radical initiated chain reaction mechanism. They proposed a mechanism in which OH radical attacked TCE in the process of Cl radical formation.[22] In studies of gas-phase TCE photooxidation using porous TiO_2 pellets, Anderson *et al.*[33] concluded that the Cl radical chain reaction constituted a minor reaction pathway to produce DCAC when low surface area TiO_2 catalysts were employed. Recently, Fan *et al.*[19] reevaluated the role of O_2^- radical and concluded that it served as the major oxidizing agent of TCE over a powdered TiO_2 catalyst. DCAC was identified as a major reaction intermediate in their study. When $H_2{}^{18}O$ was used as a coreactant, ^{18}O was not incorporated into any of the products, which prompted the authors to rule out the possibility that a OH radical mechanism was dominant.[19]

As reviewed above, precise identification and characterization of the reaction intermediates formed during the photocatalytic reaction of TCE is critical for the determination of reaction mechanisms. For the detection of chemical species resulting from TCE oxidation, most of the previous studies utilized analytical methods such as GC, GC/MS, FT-IR, MS, or trapping agents for the detection of chlorinated compounds and CO_2. Inhibition of further reactions during sampling was unavoidable in many cases. In some cases, *in situ* detection of intermediates without interruption of the reaction was employed using FT-IR spectroscopy.[19,30,36] While sensitive, FT-IR methods exhibit difficulties in direct quantitation, and although this can be avoided by the complimentary use of GC/MS,[22,23] careful and separate calibration runs for each intermediate are necessary.

Recently, with an attempt to resolve some of the issues discussed above and to provide complementary information for understanding the complex surface chemistry, we introduced a new approach to the study of photocatalytic reactions, namely *in situ* solid-state nuclear magnetic resonance (SSNMR) spectroscopy.[18] SSNMR techniques, particularly *in situ* methods,[43,44] have played an invaluable role in the study of a broad range of issues involved in heterogeneous catalysis due to the wealth of structural and dynamical information available via NMR. As described in our previous work, *in situ* SSNMR is useful in exploring the complex reaction chemistry of TCE both in the gas-phase and on the catalyst surface during the course of the reaction due to its atomic specificity, high resolution, and quantitative capabilities. Several new reaction intermediates were identified, and a number of the important intermediates that had previously been observed in other studies were evident in the spectra and could be quantified.[18] In this paper, we report our more detailed studies on the photocatalytic oxidation of TCE under several different reaction conditions. In particular, we have focused on the formation and evolution of surface-bound species on TiO_2 catalysts. By elucidating the structures of all of our observed reaction intermediates involved during the TCE photodegradation we have additional information on the reaction mechanisms. Finally, a comparison of the photocatalytic reactions over several catalysts allows us to draw some conclusions regarding the surface chemistry of TCE.

II. Materials and Methods

A. Catalyst Preparation. Photocatalytic oxidation reactions were carried out in sealed glass NMR tubes at room temperature. Catalyst samples consisting of approximately 180 mg of TiO_2 powder[45] were packed into 5 mm glass NMR tubes (Norell), which were then attached to a gas manifold. The powder was first evacuated at 773 K for 4 h to remove both weakly and strongly adsorbed water molecules as well as the majority of surface hydroxyl groups and then calcined at 773 K in a ceramic heater under 1 atm of O_2 gas for another 4 h. Typically, the O_2 was pumped out and replaced with fresh O_2 twice during calcination. Evacuation down to 2×10^{-5} Torr was followed by cooling the

(26) Lichtin, N. N.; Avudaithai, M. *Res. Chem. Intermed.* **1994**, *20*, 755.
(27) Luo, Y.; Ollis, D. F. *J. Catal.* **1996**, *163*, 1.
(28) Dibble, L. A.; Raupp, G. B. *Catal. Lett.* **1990**, *4*, 345.
(29) Dibble, L. A.; Raupp, G. B. *Environ. Sci. Technol.* **1992**, *26*, 492.
(30) Phillips, L. A.; Raupp, G. B. *J. Mol. Catal.* **1992**, *77*, 297.
(31) Yamazaki-Nishida, S.; Cervera-March, S.; Nagano, K. J.; Anderson, M. A.; Hori, K. *J. Phys. Chem.* **1995**, *99*, 15814.
(32) Yamazaki-Nishida, S.; Nagano, K. J.; Phillips, L. A.; Cervera-March, S.; Anderson, M. A. *J. Photochem. Photobiol. A:Chem.* **1993**, *70*, 95.
(33) Yamazaki-Nishia. S.; Fu, X.; Anderson, M. A.; Hori, K. *J. Photochem. Photobiol. A: Chem.* **1996**, *97*, 175.
(34) Annapragada, R.; Leet, R.; Changrani, R.; Raupp, G. B. *Environ. Sci. Technol.* **1997**, *31*, 1898.
(35) In *Photocatalytic Purification and Treatment of Water and Air*; Ollis, D. F., Al-Ekabi, H., Eds.; Elsevier: Amsterdam, 1993. (a) Holden, W.; Marcellino, A.; Valic, D.; Weedon, A. C. p 393. (b) Nimlos, M. R.; Jacoby, W. A.; Blake, D. M.; Milne, T. A. p 387. (c) Anderson, M. A.; Yamazaki-Nishida, S.; Cervera-March, S. p 405. (d) Al-Ekabi, H.; Butters, B.; Holden, W.; Powell, T.; Story, J. p 719.
(36) Driessen, M. D.; Goodman, A. L.; Miller, T. M.; Zaharias, G. A.; Grassian *J. Phys. Chem. B* **1998**, *102*, 549.
(37) Wang, C.-B.; Zhang, W.-X. *Environ. Sci. Technol.* **1997**, *31*, 2154.
(38) Wilson, J. T.; Wilson, B. H. *Appl. Environ. Microbiol.* **1985**, *49*, 242.
(39) Hopkins, G. D.; McCarty, P. L. *Environ. Sci. Technol.* **1995**, *29*, 1628.
(40) McCarty, P. L. *Science* **1997**, *276*, 1521.
(41) Newman, L. A.; Strand, S. E.; Choe, N.; Duffy, J.; Ekuan, G.; Ruszaj, M.; Shurtleff, B. B.; Wilmoth, J.; Heilman, P.; Gordon, M. P. *Environ. Sci. Technol.* **1997**, *31*, 1062.
(42) Turchi, C. S.; Ollis, D. F. *J. Catal.* **1990**, *122*, 178.
(43) Haw, J. F. In *NMR techniques in catalysis*; Bell, A. T., Pines, A., Eds.; Marcel Dekker, Inc.: New York, 1994; p 139.
(44) Haw, J. F.; Nicholas, J. B.; Xu, T.; Beck, L. W.; Ferguson, D. B. *Acc. Chem. Res.* **1996**, *29*, 259.

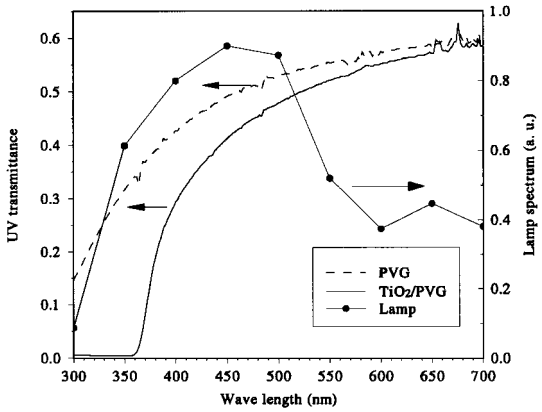

Figure 1. UV transmittance spectra of PVG (dotted curve) and a TiO_2/PVG catalyst (solid curve). A spectrum (solid circles) of the light from the Xe arc lamp acquired at the output of the quartz rod is also shown.

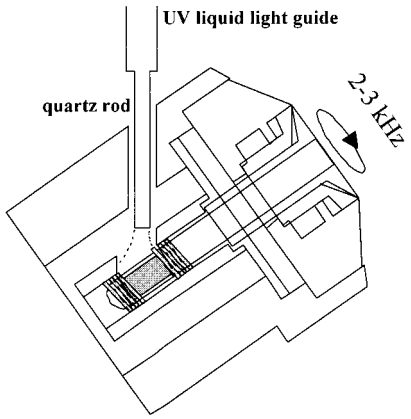

Figure 2. Schematic diagram of the *in situ* optical/MAS NMR probe head used in the present study.

powdered sample to room temperature in the heater. ^{13}C labeled TCE (Cambridge Isotope Laboratories) was then introduced into the gas manifold, and frozen onto the calcined TiO_2 powder using a liquid nitrogen trap. The amount of TCE used was routinely 48 μmol. O_2 (60 μmol) was subsequently loaded onto the sample, and the NMR tube was sealed off 10−12 mm above the catalyst sample.

A second TiO_2 catalyst was prepared by dispersing TiO_2 (with coverage of a monolayer) on the surface of transparent porous Vycor glass (PVG). The preparation method of supported monolayer TiO_2 catalysts has been established by Anpo *et al.*[46−48] As depicted in eq 1,

$$2\,(\text{-O})_3\text{Si-OH} + \text{TiCl}_4 \rightarrow (\,(\text{-O})_3\text{Si-O-})_2\text{TiCl}_2 + 2\text{HCl}$$

$$\xrightarrow{\text{hydrolysis}} \quad \begin{matrix} & \text{Si}-\text{O} & \\ \text{O} & & \text{Ti} \\ & \text{Si}-\text{O} & \end{matrix} \begin{matrix} \text{OH} \\ \\ \text{OH} \end{matrix} \qquad (1)$$

the catalyst was prepared from the gas phase hydrolysis of $TiCl_4$ with OH groups at the PVG surface. Typically, 88 μmol of $TiCl_4$ (Aldrich) was reacted at room temperature using a PVG rod (Corning 7930, BET surface area ∼150 m^2/g, pore diameter 40 Å), that was 3.6 mm in diameter and 12 mm long, weighed 180 mg, and had been previously degassed and calcined at 773 K for 4 h each. Since the saturated vapor pressure of $TiCl_4$ (11 Torr) corresponds to 88 μmol in our gas rack, typically four reaction cycles were used to insure the complete reaction of all the surface OH groups with $TiCl_4$. HCl gas produced from the reaction was completely evacuated and another loading of 88 μmol of $TiCl_4$ followed. The anchoring process was modified by controlling the amount of $TiCl_4$ introduced for different coverages, and the whole process could be repeated to create multilayer coverages. After anchoring, the catalyst was hydrated, degassed, and calcined under O_2 at 773 K. The UV−visible transmission spectrum (see Figure 1) of the TiO_2/PVG catalyst exhibited a strong absorption starting around 370 nm, which is characteristic of TiO_2 dispersed on PVG.[46] PVG displays a similarly strong absorption at much shorter wavelengths. Nevertheless, it is possible to irradiate this catalyst in a homogeneous fashion, such that the near UV light can penetrate the entire catalyst. For the MAS NMR experiments, both ends of the PVG rod were fitted with plastic end caps whose outer diameter was adjusted to fit snugly against the inner wall of the NMR tube. In this way, the sealed NMR tubes could be spun at speeds as high as 2.7 kHz.

B. NMR Methods. For the *in situ* NMR experiments, a home-built NMR probe based on a design by Gay[49] was constructed. A light pipe was incorporated into the probe to bring the near UV light to the sample through a 10 mm gap in the radio frequency coil. Figure 2 shows a schematic diagram of the probe head. The optical/MAS NMR probe is doubly tuned for ^1H and ^{13}C observation at frequencies of 300 and 75.4 MHz, respectively. A 300 W Xe arc lamp (ILC Technology) was used as the UV light source. Near infrared light produced by the lamp was filtered by a dichroic mirror (Oriel Corp.), and the remaining near UV light was delivered to the sample region inside the magnet using a liquid-filled optical light guide (Oriel Corp.) that had a polished 70 mm long suprasil quartz rod attached to its end. The quartz rod reduced the effects of radio frequency pickup by the probe coil from the aluminum-encased liquid-light guide. The light quickly diverges from the quartz rod to cover the entire sample region. The light spectrum obtained at the output of the quartz rod is displayed in Figure 1. The spectrum indicates that light used in this study ranges in wavelength from 350 to 550 nm and its maximum matches the onset of the absorption region for the TiO_2/PVG catalyst. The near UV light power that reaches the sample was measured to be 5 mW by standard ferrioxalate actinometry.[50]

Results and Discussion

A. Photocatalytic Oxidation of TCE on the TiO_2 Powder Catalyst. Figure 3a shows proton-decoupled ^{13}C MAS NMR spectra obtained during the *in situ* photooxidation of TCE in the presence of O_2 and the powdered TiO_2 catalyst. Similar results were observed and reported earlier.[18] The narrow line widths of the peaks indicate that these species are very mobile and most likely exchange rapidly between the surface and the gas phase. Typically each NMR spectrum consists of the average of 48 transients that were obtained with a delay time of 4 s between acquisitions, such that the time evolution could be monitored on the time scale of a few minutes. The ^{13}C spin−lattice relaxation times were measured to be between 0.7 and 1.2 s for all of the mobile species, with the exception of phosgene, which has a T_1 of 2.3 s. NMR spectra collected as a function of UV irradiation time show the degradation of TCE and creation of a number of long-lived intermediates, including carbon monoxide (CO), DCAC, phosgene, and pentachloroethane (C_2HCl_5), and their conversion to the final products CO_2 and phosgene. Assignment of these intermediates is confirmed by comparing ^{13}C NMR shifts for liquid samples reported in the literature[51] or prepared in our lab and by taking proton coupled spectra during the photoreactions. The fact that TCE

(45) TiO_2 P-25 powdered catalyst is a gift from Degussa Corp. The P-25 has roughly 70% anatase and a surface area of ∼50 m^2/g.

(46) Anpo, M. Aikawa, N.; Kubokawa, Y.; Che, M.; Louis, C.; Giamello, E. *J. Phys. Chem.* **1985**, *89*, 5017.

(47) Yamashita, H.; Ichihashi, Y.; Harada, M.;Stewart, G.; Fox, M. A.; Anpo, M. *J. Catal.* **1996**, *158*, 97.

(48) Osipenkova, O. V.; Malkov, A. A.; Malygin, A. A. *Russ. J. General Chem.* **1994**, *64*, 498.

(49) Gay, I. D. *J. Magn. Reson.* **1984**, *58*, 413.

(50) Hatchard, C. G.; Parker, C. A. *Proc. Royal Soc. London* **1956**, *A235*, 518.

(51) *Stadtler Standard Carbon-13 NMR spectra* Bio-Rad Laboratories: Philadelphia, PA, 1994.

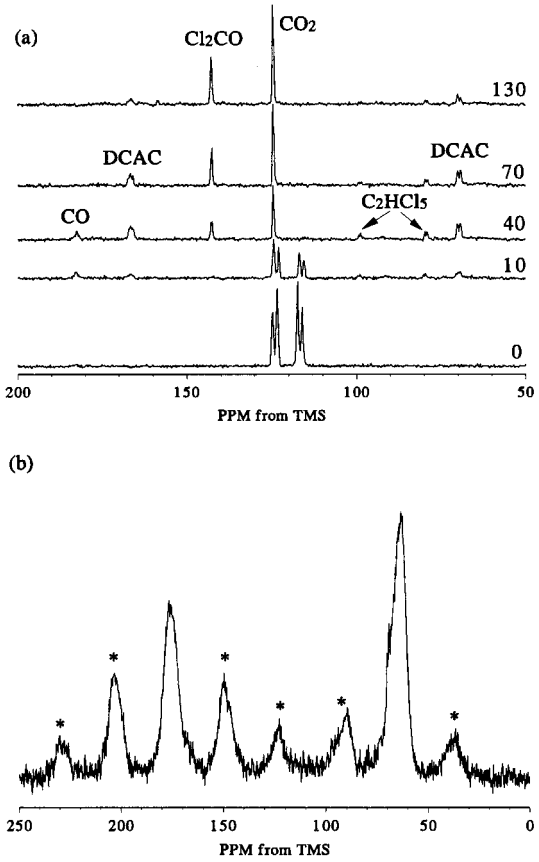

Figure 3. (a) Proton-decoupled ^{13}C MAS NMR spectra obtained during the photocatalytic oxidation of 48 μmol of TCE and 60 μmol of O_2 on the Degussa P-25 TiO_2 powdered catalyst. The UV irradiation time is indicated in min. (b) A spectrum obtained with $^1H-^{13}C$ cross polarization (contact time 3 ms) recorded after the UV light was turned off. The vertical scale of the spectrum (b) is expanded 10× compared to the spectra in (a). The asterisks indicate spinning sidebands of surface-bound dichloroacetate.

oxidation leads to the creation of intermediates/products containing at most one hydrogen atom aided in the peak assignments. The chemical shifts and *J* couplings of the observed compounds are compiled in Table 1. Most of the carbon containing intermediates identified by SSNMR in the reaction with the powdered catalyst are in good agreement with those observed in previous gas phase photooxidation studies of TCE using several different types of TiO_2 photoreactors.[19−23,35a,b,36] However, there was no indication of the formation of mono- or dichloroacetaldehyde observed in previous liquid phase[11,14] or other gas phase reaction studies in a similar packed catalyst bed reactor.[31,32,35c] The surface water content in these experiments was extremely low since the powder was evacuated at 773 K. The ^1H NMR MAS spectrum (not shown) obtained for this sample showed no indication of H_2O although a very small and broad peak was observed that is due to surface OH groups.

A carbon balance obtained by integrating the peak areas of the spectra shown in Figure 3a indicates a significant loss of signal (up to 50%) from the original TCE concentration after 50 min of UV irradiation. Therefore, an extended accumulation with a longer delay time (20 s) was obtained immediately after ceasing UV irradiation. Broad peaks with low intensities were observed at the base of the narrow lines, and these broad resonances are responsible for the apparent loss of signal.[18] In order to characterize the broad components, a separate spectrum was obtained using $^1H-^{13}C$ cross polarization (CP), and this spectrum is displayed in Figure 3b. The spectrum shows two broad resonances at 64.0 and 177.3 ppm and a number of spinning sidebands indicated by asterisks. This result provides definitive evidence for the presence of surface-bound species. The integrated signal intensities of the two isotropic resonances and their associated side bands are very nearly the same, indicating the formation of a single surface species containing two carbon atoms. We have identified this species as dichloroacetate (Cl_2CHCOO^-), which presumably forms from the reaction of DCAC with surface hydroxyl groups. The assignment is based on the fact that the spinning sidebands show chemical shift anisotropy patterns characteristic of a methyl carbon and a carbonyl carbon. The proton-coupled ^{13}C CP/MAS (contact time 50 μs) spectrum (not shown) displayed a number of spinning sidebands, which outline a Pake doublet powder pattern that is characteristic of an isolated $^{13}C-H$ spin pair. This Pake pattern is centered at 64.0 ppm, indicating that the methyl carbon has one attached proton. The chemical shift of the carbonyl carbon (177.3 ppm) is somewhat high compared to the chemical shift of dichloroacetic acid in liquid (63.8 and 170.0 ppm).[51] Such a shift to down field might be associated with acetate bond formation of the carbonyl carbon to titanium sites on the catalyst surface. Continued UV irradiation did not break up dichloroacetate, while the other, more mobile species were converted into phosgene and CO_2. These results as well as the results of detailed experiments on the fate of dichloroacetate on the TiO_2/PVG catalyst (see section III.B.2. below) clearly indicate that some reaction intermediates such as DCAC move to dark regions of the catalyst and react to form stable, strongly surface-bound species.

In addition to the formation of dichloroacetate, the photooxidation of TCE on the powdered TiO_2 catalyst did not lead to complete mineralization since phosgene did not oxidize further under dry conditions even after continued UV irradiation. In order to investigate whether phosgene could be converted thermally to CO_2, the sample was heated after the UV irradiation. ^{13}C MAS NMR measurements were followed after the sample was heated at 373 K and later to 473 K for 1 h. There were no remarkable changes observed in the NMR spectrum upon heating the sample to 373 K. However, all the phosgene decomposed to produce CO, C_2Cl_4, C_2Cl_6, and CO_2 after heating at 473 K for 1 h. In similar experiments, Fan *et al.*[19] reported the conversion of phosgene to tetrachloroethylene (C_2Cl_4) on TiO_2 at 473 K. The NMR spectrum obtained after heating at 473 K also indicates that all of the pentachloroethane was converted. However, the ^{13}C CP/MAS spectrum obtained after the thermal reaction indicated that the surface-bound dichloroacetate species was not significantly affected.

Separate experiments were conducted on samples where a small quantity of water was deliberately left on the TiO_2 catalyst by carefully controlling the conditions of the evacuation step. *In situ* studies revealed that the production of dichloroacetate was somewhat diminished, and a concomitant formation of dichloroacetic acid was observed. This latter species is mobile (see section III.B.3. below), and its slow photooxidation lead to the formation of CO_2, in agreement with previous studies.[31,52] We also note that TCE photocatalysis was not observed in samples prepared without added O_2.

B. Photocatalytic Oxidation of TCE on TiO_2/PVG Catalyst. In a second series of experiments, we examined TCE photooxidation using the supported monolayer TiO_2 catalyst, which was synthesized in a manner described in section II-A above. The catalyst used in the experiments described below had a TiO_2 coverage of one monolayer. The photocatalytic

(52) Sauer, M. L.; Ollis, D. F. *J. Catal.* **1996**, *163*, 215.

Table 1. Chemical Shifts of Species Observed over TiO_2 Powder

species	chemical formula	chemical shifts (ppm) and *J* couplings[a]
trichloroethylene (TCE)	C_2HCl_3	116.7, 124.0 (J_{C-C} = 103 Hz, J_{H-C} = 201 Hz)[b]
dichloroacetyl chloride (DCAC)	C_2HCl_3O	70.0, 167.5 (J_{C-C} = 65 Hz, J_{H-C} = 186Hz)
pentachloroethane	C_2HCl_5	79.5, 100.0 (J_{C-C} = 50 Hz, J_{H-C} = 185 Hz)
carbon dioxide	CO_2	124.0
phosgene	CCl_2O	143.0
carbon monoxide	CO	183.0
dichloroacetate	$Cl_2HCCOO-Ti(O-)_3$	64.0, 177.3

[a] The error bars for the chemical shifts are ±0.5 ppm for the mobile species, ±1.0 ppm for the surface bound species, and the error bars for the *J* couplings are ±5 Hz. [b] J_{H-C2} = 12.5 Hz estimated from TCE in $CDCl_3$ but not observable in this work.

properties of TiO_2/PVG have been studied and reviewed by Anpo *et al.*[53,54] It has been observed that by dispersing TiO_2 over the PVG surface both the physical and chemical nature of TiO_2 are significantly modified with the result that the catalytic activity and selectivity can be enhanced as compared to bulk TiO_2.[53,54]

1. TCE + O_2. A number of studies of TCE photooxidation were performed under dry conditions. The TiO_2/PVG catalyst was evacuated at 773 K for 4 h and subsequently loaded with 48 μmol of TCE and 96 μmol of O_2, as before for the powdered TiO_2 catalyst.

As can be seen in the ^{13}C MAS NMR spectra shown in Figure 4a, TCE degrades quickly to form a number of intermediates including DCAC, oxalyl chloride ($Cl_2C_2O_2$), pentachloroethane, trichloroacetaldehyle (Cl_3CCHO), and trichloroacetyl chloride (Cl_3CCOCl) in a trace amount. Ultimately these species are converted to the final products phosgene and CO_2. The NMR shifts and J couplings of these intermediates are listed in Table 2. In contrast to our previous experiments involving the TiO_2/PVG catalyst with a coverage of roughly a quarter monolayer,[18] the formation of CO is not seen and the formation of Cl_3CCHO and $Cl_2C_2O_2$ is suppressed. Direct integration of the NMR peaks allows us to estimate the gradual evolution of individual species (see below).

After 230 min of UV irradiation, the extended Bloch decay spectrum (top spectrum in Figure 4b) exhibits the presence of phosgene and CO_2. CO_2 spinning sidebands are evident and indicate the presence of a small quantity of strongly adsorbed CO_2. Integration of the peaks results in CO_2:phosgene ratio of 2:1, and the total carbon balance of the mobile species was calculated to be 85% of the initial TCE concentration. There is no clear indication of the presence of surface-bound species in the Bloch decay spectrum. However, the ^{13}C CP/MAS spectrum (bottom spectrum in Figure 4b) does show the existence of at least two surface-bound species which are responsible for the minor loss in the carbon balance. We identify these species as dichloroacetate and trichloroacetate (Cl_3CCOO^-) which are bound to the surface of TiO_2/PVG via chemical bonds to both Si and Ti sites. As with the powdered catalyst, we interpret the formation of these surface species as due to the reaction of DCAC and trichloroacetyl chloride with surface OH groups. As seen in Figure 4b, the spectrum is very complex due to overlapping resonances of the carbonyl groups on Ti sites and Si sites as well as their spinning sidebands. Assignments (see Table 2) were made by comparing the chemical shifts of surface-bound species observed on the powdered TiO_2 surface with those on the SiO_2 (pure PVG), as will be discussed below. The chemical shifts of dichloroacetate bound to Ti sites are found to be 63.7 and 175.0 ppm for the methyl and carbonyl resonances, respectively, which are very close to those observed on the TiO_2 powder surface. The other pair of chemical shifts found in this experiment (63.7 and 162.1 ppm) is assigned to dichloroacetate bound to Si sites on the surface (see below for a description of dichloroacetate formation on pure PVG). The chemical shift of the carbonyl carbon of trichloroacetate shows the similar upfield shift in going from Ti (171.0 ppm) to Si (159.1 ppm) sites as does dichloroacetate. Although the TiO_2/PVG was prepared using an excess amount of $TiCl_4$ in order to produce a full monolayer coverage of titanium dioxide, this result indicates that there are some SiO_2 surface sites that remain. Nevertheless, it is possible that DCAC reacts preferentially with $(-O)_3SiOH$, so that quantitation of the relative numbers of Ti and Si sites is not possible at this time. The signal from surface adsorbed CO_2 is also enhanced via cross polarization (from H atoms in surface OH groups) in the CP/MAS spectrum.

^1H MAS NMR spectra were also collected and show the presence of TCE and surface OH groups (see Figure 4c). The intensity ratio of [TCE]/[OH] was calculated to be ~0.5 in the dry sample. ^1H MAS NMR spectra show the destruction of TCE (6.4 ppm) and formation of DCAC (6.2 ppm). Although not evident in Figure 4c Cl_3CCHO was found to resonate at ~9.0 ppm in a separate experiment. The ^1H NMR spectra taken during the reaction also indicate no significant loss of surface hydroxyl groups, suggesting that OH groups do not participate in TCE oxidation process to a significant extent. The consumption of OH groups in photocatalytic oxidation reactions has been a subject of some controversy. From the *in situ* FT-IR measurements of TCE photooxidation, Raupp *et al.*[30] observed the consumption of water or/and surface hydroxyls on untreated TiO_2 surface, while Fan *et al.*[19] reported no OH consumption on a TiO_2 surface. Production of HCl is anticipated but not resolved by ^1H NMR (see Figure 4c). However, slight downfield shifts (~1 ppm) of the OH peak are observed, indicating an increased acidity of the surface protons, which is therefore suggestive of the adsorption of some HCl.[55] Formation of gas-phase HCl in the reaction was confirmed using FT-IR. For this measurement, we placed the NMR sample which had been previously irradiated with UV light into a test tube with an iron ball. The tube was evacuated down to 2×10^{-5} Torr, after which the NMR sample was opened using the iron ball. All the products in gas phase were transferred into a pre-evacuated cell for the FT-IR measurement. The FT-IR spectrum (not shown) clearly reveals the presence of CO_2 and phosgene as well as HCl.

2. Reaction of Surface Bound Species on TiO_2/PVG. From the photodegradation study of TCE on the TiO_2 powder (see Part III.A., above), further degradation of dichloroacetate formed in the dark regions of the powder was impossible.

(53) Anpo. M. *Res. Chem. Intermed.* **1989**, *11*, 67.
(54) Anpo, M.; Yamashita, H. In *Surface Photochemistry*; Anpo. M., Ed.; John Wiley & Sons: New York, 1996; p 117.
(55) Pfeifer, H. In *Solid-State NMR II: Inorganic Matter*; Diehl, F., Gunther, H., Kosfeld, R., Seeling, J., Eds.; Springer-Verlag: Berlin, 1994; p 33.

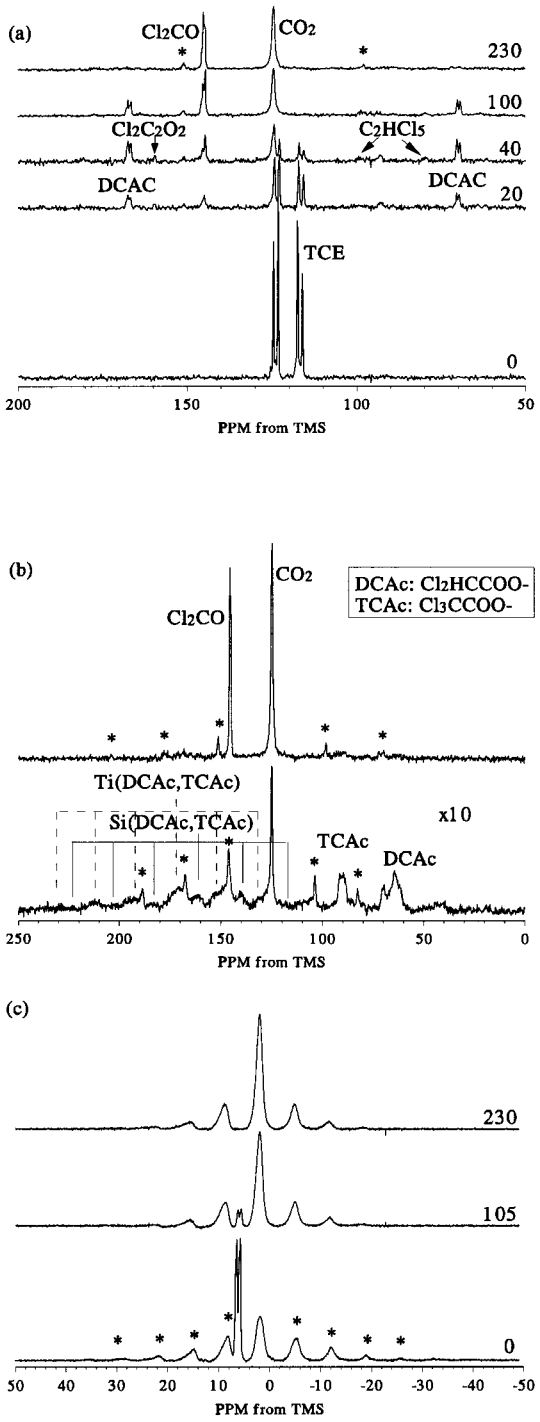

Figure 4. MAS NMR spectra obtained during the *in situ* photooxidation of TCE on the TiO_2/PVG catalyst. The spinning rate was 2.0 kHz. (a) Proton-decoupled ^{13}C spectra acquired during UV irradiation. (b) A ^{13}C spectrum obtained with extended accumulation (top) and a ^{13}C CP/MAS (contact time 3 ms, bottom) after the lamp was turned off. The asterisks indicate spinning sidebands of strongly adsorbed CO_2. (c) ^1H MAS NMR spectra acquired during photooxidation (probe ^1H background subtracted). Abbreviations: dichloroacetate (DCAc); trichloroacetate (TCAc).

However, dichloroacetate formation on the TiO_2/PVG surface was suppressed in the presence of UV light. Since it was not clear whether dichloroacetate, once formed on the catalyst surface, could be photodegraded, we examined the reactivity of dichloroacetate by using an experimental setup as described below.

(1) A NMR sample was prepared by loading 48 μmol of TCE and 24 μmol of O_2 on the surface of completely dried TiO_2/PVG.

(2) UV irradiation was continued until there was no more degradation of TCE observed. The O_2 deficiency prevented further degradation, in accordance with the stoichiometry of the following TCE oxidation reaction

$$3Cl_2C{=}CHCl + 5O_2 \rightarrow 4CO_2 + 3HCl + 2COCl_2 + Cl_2$$

which is in accordance with our observed 2:1 ratio of CO_2: phosgene. Note that it is possible to write reactions which do not result in Cl_2 production, but these change the relative ratio of CO_2 and phosgene or involve H_2O as a reactant. A ^{13}C MAS spectrum acquired after 92 min of UV irradiation is displayed in Figure 5a and reveals the formation of DCAC, phosgene, pentachloroethane, Cl_3CCHO, and CO as well as unreacted TCE.

(3) The sample was stored in the dark for 28 days to allow the reaction of DCAC with surface OH groups to proceed. A spectrum shown in Figure 5b clearly indicates the growth of broad resonances during the dark period while the DCAC peaks decreased markedly. The concentration of phosgene also decreased most likely due to its reaction with surface OH groups to form CO_2 and HCl.

(4) The sample was then heated at 423 K for 30 min to complete the hydrolysis of the remaining DCAC. Figure 5c shows the resulting NMR spectrum, which reveals the further increase in intensity of broad peaks that result from the consumption of DCAC. Additional phosgene was also consumed. It is also possible to associate at least some of the decreased phosgene concentration with the formation of another surface bound species, which may be chloroformate ($ClCOO^-$) that is produced via reaction of phosgene with surface OH groups (see below).

(5) After heating, the NMR sample was broken and the volatile species were released. The catalyst was then transferred to a fresh NMR tube and evacuated to a pressure of 2×10^{-5} Torr. O_2 (96 μmol) was loaded, and the sample was again sealed. The ^{13}C Bloch decay (Figure 5d) and CP/MAS (Figure 5f) spectra acquired at this stage of the experiment are shown. The Bloch decay spectrum clearly shows the removal of all gas phase species after evacuation, while the CP/MAS spectrum indicates the presence of the surface-bound dichloroacetate both on Ti sites (63.7 and 175.0 ppm) and on Si sites (63.7 and 162.1 ppm). Significant differences in chemical shift for the carbonyl carbons in dichloroacetate adsorbed on the two different metal sites are evident, while the chemical shifts of the methyl carbons adsorbed on both sites are found to be essentially identical. These dichloroacetate resonances also appear to be narrower than the corresponding signals on the TiO_2 powder (see Figure 3c), suggesting that the surface sites on the TiO_2/PVG sample are more homogeneous.[53,54]

(6) As the final step, *in situ* NMR observation was made during UV irradiation of the sample. The degradation of dichloroacetate did occur, although the reaction rate was much slower than that observed for TCE. NMR measurements made after a UV irradiation time of 310 min are shown in Figure 5 parts e and g for the Bloch decay and CP/MAS experiments, respectively. From both spectra, it is evident that upon UV irradiation most of the dichloroacetate is decomposed to form phosgene and CO_2. After 310 min of irradiation, destruction of dichloroacetate was complete as indicated by the disappearance of the methyl carbon peak at 63.7 ppm. A very small signal corresponding to the formation of trichloroacetate (92.1

Table 2. Additional Observed Species from TiO_2/PVG Catalysts

species	chemical formula	chemical shifts (ppm)
dichloroactic acid	$C_2H_2Cl_2O_2$	63.0, 167.5 (J_{C-C} = 66 Hz)
chloroform	$CHCl_3$	77.2
oxalyl chloride	$C_2Cl_2O_2$	159.0
trichloroacetaldehyde	C_2HCl_3O	93.0, 177.0 (J_{C-C} = 44 Hz, J_{H-C} = 195 Hz)
trichloroacetyl chloride	C_2Cl_4O	94.0, 164.0 (J_{C-C} = 75 Hz)
trichloroacetic acid	$C_2HCl_3O_2$	88.0, 164.0 (J_{C-C} = 80 Hz)
dichloroacetate	Cl_2HCCOO-$Si(O\text{-})_3$	63.7, 162.1
dichloroacetate	Cl_2HCCOO-$Ti(O\text{-})_3$	63.7, 175.0
trichloroacetate	Cl_3CCOO-$Si(O\text{-})_3$	89.2, 159.1
trichloroacetate	Cl_3CCOO-$Ti(O\text{-})_3$	92.1, 171.0

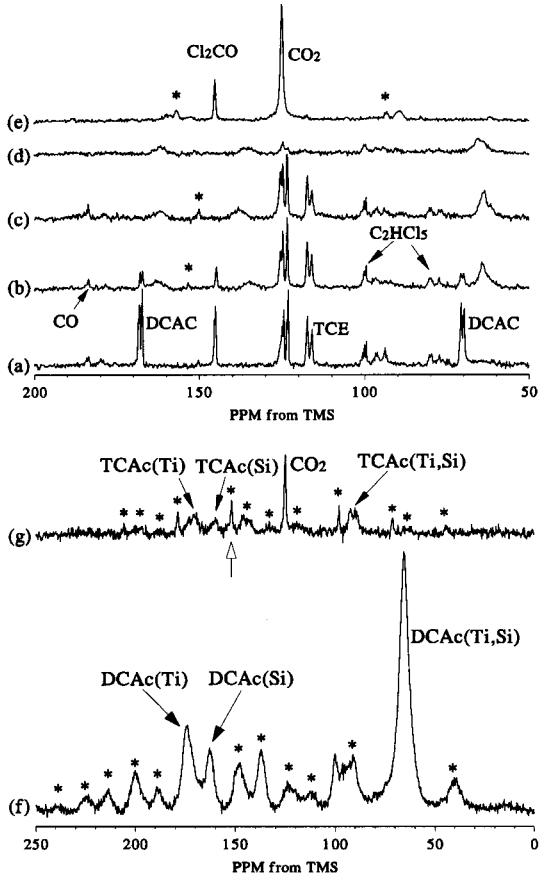

Figure 5. Proton decoupled ^{13}C MAS and CP/MAS spectra acquired during the photocatalytic and dark reaction steps as described in the text. Bloch decay spectra: (a) after UV irradiation for 92 min; (b) after dark reaction for 28 days; (c) after heating at 423 K for 30 min; (d) after evacuation at room temperature; (e) after UV irradiation for 310 min; CP/MAS spectra (contact time 3 ms): (f) same conditions as (d); (g) same conditions as (e). Abbreviations: dichloroacetate (DCAc); Trichloroacetate (TCAc).

and 171.0 ppm for trichloroacetate bound to Ti sites, 89.2 and 159.1 ppm for trichloroacetate bound to Si sites) was observed, and their intensities were found to increase slowly as the irradiation time increased. Further irradiation for 90 more min did not affect the signal intensities of trichloroacetate on either site. *This result indicates that trichloroacetate, once formed from DCAc, is very resistive to further destruction, both when bound to Ti and to Si sites on the catalyst*. Finally, a peak appearing at 152 ppm (underneath a sharp CO_2 spinning sideband) was observed and is indicated by an open arrow in Figure 5g. The chemical shift of this peak could correspond to either CO_3^- or $ClCOO^-$ on the surface.

The experimental results described in this section demonstrate that once formed, DCAC reacts with surface hydroxyl groups to form surface-bound dichloroacetate in a dark reaction, while continuous irradiation breaks down the dichloroacetate to form phosgene and CO_2 at the surface of the TiO_2/PVG catalyst. The results also imply that the formation of phosgene during the photooxidation of TCE primarily originates from photooxidation of DCAC, supporting previous findings by Jacoby *et al.*[22,23] According to their report, phosgene and CO are formed in approximately equimolar amounts from DCAC. The production of CO was not observed in our *in situ* NMR study of dichloroacetate photodegradation.

3. TCE + O_2 + H_2O. The influence of water on the photooxidation of TCE was investigated by introducing H_2O (0.1 mmol) before TCE (48 μmol) and O_2 (96 μmol) were loaded onto the TiO_2/PVG catalyst. ^1H NMR spin counting was used to quantify the amount of H_2O adsorbed on the catalyst surface before the reaction was initiated. The surface water content was determined to be roughly equivalent to one monolayer coverage. The observed ^1H line width of 700 Hz indicates that this water is strongly associated with surface hydroxyl groups and very likely evenly distributed over the surface of the 40 Å pores of the catalyst. Figure 6a shows the resulting ^{13}C MAS NMR spectra as a function of UV irradiation time, while Figure 6b shows a kinetic plot from direct integration of peak areas shown in Figure 6a. As shown in Figure 6, degradation of TCE upon UV illumination occurs in a very similar fashion to that observed under dry conditions. However, the formation of dichloroacetic acid (63.0 and 167.5 ppm) as a major intermediate is observed. Narrow NMR line widths for dichloroacetic acid indicate that it is very mobile over the hydrated surface or may be in fast exchange with the gas phase. The carbonyl carbons in both DCAC and dichloroacetic acid were found to resonate at the same chemical shift, 167.5 ppm (see Figure 6a). Once formed, dichloroacetic acid could be further photooxidized, but its degradation rate was slow. Formation of phosgene is almost suppressed in the presence of surface water, in good agreement with a previous report.[19] CO, Cl_3CCHO, and $Cl_2C_2O_2$ are not found under these conditions. However, small quantities of DCAC are observed at an early stage during the UV irradiation. A second experiment was run with roughly half the amount of adsorbed water. Formation of DCAC was predominant at the early stage of UV illumination, while dichloroacetic acid was produced with a concomitant decrease in the amount of DCAC during the photoreaction. From these results, it is evident that the destruction of TCE leads to formation of DCAC and immediate hydrolysis of DCAC follows to form dichloroacetic acid.[19,33,35a] It is not clear at this point whether phosgene formation is suppressed due to the presence of water or whether phosgene is efficiently decomposed as soon as it forms under hydrated conditions. However, phosgene is known to react with water to yield CO_2 and HCl,[56] and therefore the latter case is more plausible.

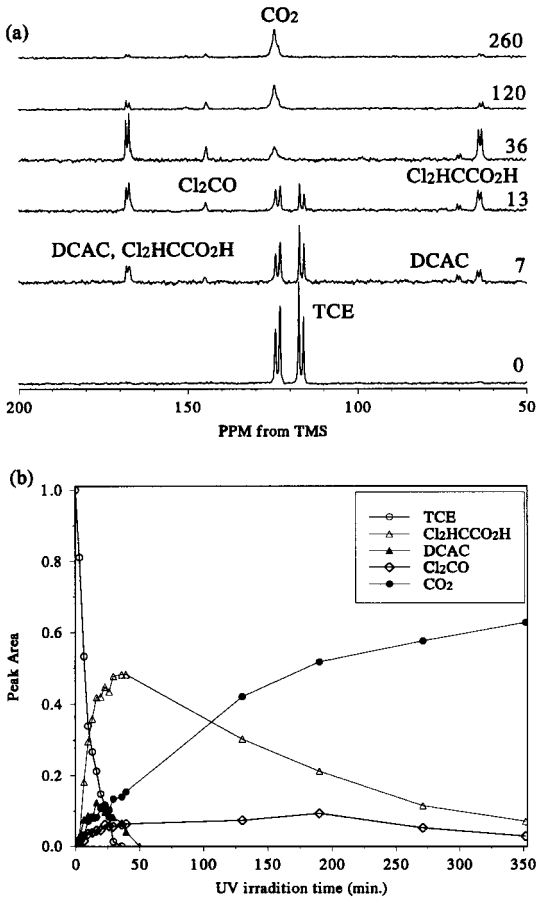

Figure 6. (a) Proton-decoupled ^{13}C MAS spectra obtained during TCE photocatalytic degradation with O_2 and H_2O as coreactants over the TiO_2/PVG catalyst. (b) The resulting kinetic plot obtained by integration of the spectra in (a).

4. TCE + H_2O. Hydrated samples were prepared by fully saturating the catalyst with water followed by evacuation for 30 min at room temperature. TCE (48 μmol) was used as before. ^{13}C MAS NMR spectra (not shown) were acquired during UV irradiation for a period of 2 h. There was no indication of any TCE degradation. In addition, the thermal reaction of TCE in the presence of the catalyst and adsorbed water was examined by heating the same sample at 423 K for an hour. We did not observe any change in ^{13}C MAS NMR spectrum. Anpo *et al.*[46,53,54,57] have reported the photocatalytic hydrogenolysis of unsaturated hydrocarbons (alkenes and alkynes) and the photocatalytic isomerization of alkenes on both TiO_2 powder catalysts and TiO_2/PVG catalysts. In their studies of photocatalytic hydrogenolysis, reactions were run in the presence of H_2O but without O_2. However, our findings indicate that the presence of O_2 is essential to initiate oxidation of TCE. It is also possible to conclude that if any OH radical is involved in the photocatalytic oxidation of TCE, the radical does not form or does not attack TCE in the absence of oxygen.

C. TCE Oxidation on PVG. The photocatalytic activity of pure Vycor glass has been reported by Anpo *et al.*[58−61] In those experiments, irradiation was performed with shorter wavelengths to compensate for the fact that PVG has an absorption maximum near 260 nm.[62] We also examined the reactions of TCE on PVG alone and used the same procedure as described above for the photooxidation of TCE on TiO_2/PVG, so that direct comparison between TiO_2/PVG and PVG systems should be possible. Figure 7 shows three ^{13}C NMR spectra obtained from these examinations, and the findings are summarized below.

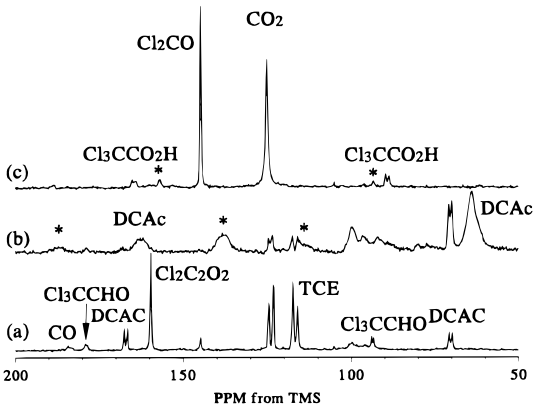

Figure 7. ^{13}C MAS NMR spectra obtained for the reaction of TCE on PVG. (a) Bloch decay spectrum acquired after UV photooxidation reaction for 20 min. (b) CP/MAS spectrum (contact time 3 ms) acquired after forming DCAc in the dark. (c) Bloch decay spectrum after UV reaction for 340 min.

Our data indicate that photooxidation reactions are possible at room temperature and result in the degradation of TCE and the formation of DCAC, $Cl_2C_2O_2$, CO, Cl_3CCHO, phosgene, and CO_2. The ^{13}C MAS NMR spectrum in Figure 7a shows the presence of these reaction intermediates and products after UV exposure for 20 min. PVG also provides surface hydroxyl groups to form surface bound dichloroacetate when DCAC is present. Figure 7b exhibits the dichloroacetate resonances (64 and 162 ppm) which are identical to the peaks assigned to dichloroacetate adsorbed on the surface of the TiO_2/PVG catalyst. Dichloroacetate on PVG is presumably bound to Si sites. When the photooxidation of dichloroacetate was examined in the presence of O_2 using the procedure described above for investigating its degradation on the TiO_2/PVG catalyst, photodegradation was observed as well as the production of phosgene and CO_2. The formation of trichloroacetate also was observed toward the end of the dichloroacetate destruction. Upon continued UV irradiation, reaction intermediates were converted to phosgene and CO_2, indicating that PVG behaves in a similar manner to the TiO_2/PVG catalyst, although the reaction rate is found to be slower than that found for TiO_2/PVG. In particular, the initial degradation rate of TCE appears to about an order of magnitude slower than for the TiO_2 catalysts. Figure 7c shows a ^{13}C MAS NMR spectrum obtained after photooxidation of TCE for 340 min. The spectrum indicates the presence of phosgene and CO_2 as final products as well as a minor concentration of trichloroacetic acid (Cl_3CCO_2H).

As can be seen in Figure 1, the spectrum of UV light we have used in these experiments has a maximum at ~450 nm with small contributions from light with wavelengths shorter than 350 nm. At the same time, the UV transmittance spectrum of PVG (degassed at 773 K) indicates that PVG starts absorbing UV light around 350 nm. A speculation that photooxidation of TCE on PVG is driven primarily by the UV photons available

(56) Morrison, R. T.; Boyd, R. N. *Organic Chemistry*; Allyn and Bacon: Boston, 1987; 5th ed., p 886.
(57) Anpo, M.; Aikawa, N.; Kodama, S.; Kubokawa, Y. *J. Phys. Chem.* **1984**, *88*, 2569.
(58) Anpo, M.; Kubokawa, Y.; Fujii, T.; Suzuki, S. *J. Phys. Chem.* **1984**, *88*, 2572.
(59) Anpo, M.; Yun, C.; Kubokawa, Y. *J. Catal.* **1980**, *61*, 267.
(60) Anpo, M. *Chem. Lett.* **1987**, 1221.
(61) Yun, C.; Anpo, M.; Kubokawa, Y. *Chem. Lett.* **1979**, 631.
(62) Anpo, M.; Yun, C.; Kubokawa, Y. *J. Chem. Soc., Faraday I* **1980**, *76*, 1014.

with wavelengths well below 350 nm led us to run another control experiment. TCE photooxidation was carried out on PVG using a 350 nm UV cutoff filter as well as an IR filter. The results obtained were very similar in terms of the observed reaction intermediates; however, the reaction rate becomes somewhat slower.

D. Discussion of the Influence of Radical Species. TCE is a very reactive species that degrades quickly in the presence of UV light and the catalytic surfaces featured in these studies. Currently, complete elucidation of the reaction mechanisms is not possible in part due to the large number of reactive radical species that are most likely present in low abundance. In addition, direct comparisons of the results from different research groups are challenging due to the large number of unique reaction conditions, different photoreactors, and analytical methods that have been used to study TCE photodegradation reactions. The NMR experiments described above shed light on a number of questions related to the photocatalytic surface chemistry of TCE. In particular, these experimental results yield information that will be useful to help resolve the following issues.

1. Involvement of O_2 versus OH in TCE Photooxidation. As discussed in the Introduction, the identity of the initiating species in photocatalytic oxidation processes has been under considerable debate. In the liquid phase, a strong case has been made for the involvement of hydroxyl radical in initiating the photodegradation process. In the gas−solid interface, formation of monochloroacetyl chloride or dichloracetaldehyde is anticipated when OH radical inserts directly into the TCE double bond.[31] However, from our observation of DCAC as the major intermediate as well as other reports[18,19,22,23,35a] it is evident that OH radical does not attack TCE directly, even though OH radical might form as a result of the interaction between the photogenerated hole and OH^-/H_2O species at the surface. If OH radicals are involved in TCE photooxidation, as proposed by Howe *et al*.,[63] their role should be defined as assisting the formation of other reactive radicals which readily attack TCE.

A common denominator in our experiments is the observed reactivity of TCE over the surfaces of TiO_2 powder, TiO_2/PVG, and PVG employed. According to previous studies,[5,6,53,54,63] one possible process which can occur at all of these surfaces is the creation of $[Ti^{3+}-O^-]$ or $[Si^{3+}-O^-]$ species due to charge transfer upon UV illumination. Observed radical species common to the three different surfaces[5,6,53,54,64] are O_2^-, O^-, and O_3^-. We anticipate that O_2 or oxygen radicals forming from electronic activation on the surface act as the TCE-attacking species. O_2^- is known to be the most stable thermally among these radicals.[65] Insertion of one of these radicals into the TCE double bond can be suggested as the radical initiation step. As a result of the insertion, formation of DCAC is expected to occur although the detailed reaction steps in this process are not evident in our present study. Since O_2 is necessary to break down dichloroacetate, further destruction of DCAC which leads to the formation of phosgene and CO_2 is also expected to involve oxygen radical species. However, in this case, the question of the role of TiO_2 arises. Anpo *et al.* have associated the photocatalytic activity of PVG with formation of $[Si^{3+}-O^-]$ surface site as a result of charge transfer.[61] Our observations of the same reaction intermediates on both bare PVG and TiO_2/PVG indicate that the same or at least similar initiating species are involved. In fact, the titanium oxide species dispersed on PVG might just assist the photooxidation of TCE on the surface. The assistance becomes possible by providing surface sites which can form $[Ti^{3+}-O^-]$ species. These active sites will be created by absorbing UV light with longer wavelength (∼50 nm) in comparison with the wavelength needed in PVG (SiO_2). Note that the TiO_2 surface was the most effective in terms of the observed initial rates of degradation.

2. Involvement of Cl Radical. It is also evident that Cl radicals play an important role in the TCE photodegradation. Most of the reaction intermediates need to involve either Cl addition or loss of Cl radicals. For example, the formation of pentachloroethane is postulated to take place by the addition of two Cl radicals to TCE. Formation of trichloroacetyl chloride and trichloroacetate most likely takes place as a result of H atom abstraction and an addition of Cl radical to DCAC and dichloroacetate, respectively. The photosensitizing effect recently observed in mixtures of TCE with other organic pollutants also supports a mechanism involving Cl radicals.[24,26,27] However, a reaction pathway proposed by Nimlos *et al*.[22] which associates the direct attack of Cl radical on the TCE double bond still needs to be proved. While a Cl radical chain reaction mechanism can explain the formation of DCAC and phosgene, in early studies[8−10] the complete mineralization of TCE was never observed nor were the yields of CO_2 production very high even after long UV irradiation times. In addition, we[18] and others[19] have observed the necessity of O_2 as a reagent in order to initiate the TCE photocatalysis. As noted in section III.B.2, insufficient O_2 caused the degradation of TCE to be incomplete. The Cl radical mechanism is therefore not sufficient to explain the complete mechanisms of TCE degradation reactions as observed by ourselves and others, although the addition of Cl-containing reagents as a source of Cl radicals has been observed to increase the reaction rate in the degradation of nonhalogenated species.[66] Our observed quantum yields (as measured from the degradation of TCE within 20 min using 5 mW of UV light) corresponds to roughly 100% which represents a high yield, but it is not as high as the value of $\Phi \sim 100$ reported by Bertrand *et al*.[8] The propagation of Cl radical chain reactions may be dependent on a number of factors related to experimental conditions.

3. Reaction Pathways for Degradation of DCAc. The photodegradation of the surface-bound dichloroacetate species is considered to proceed via an attack of oxygen radicals such as O_2^- or O^-. In our examination of the dichloroacetate degradation using *in situ* NMR, we did not observe the formation of any gas phase species other than phosgene and CO_2. It is also evident that dichloroacetate breaks down while it is bound to the surface rather than desorbing from the surface prior to degradation.

Our finding that trichloroacetyl chloride and trichloroacetate are both very resistive to further oxidation indicates that the abstraction of a chlorine atom from these reaction intermediates as well as other species is either not possible or extremely slow. We expect that trichloroacetyl chloride, trichloroacetate, and, to a somewhat lesser extent, dichloroacetate [27,52] play a primary role in catalyst deactivation processes, although the formation of these species may be inhibited by hydration.

Finally, we reported[18] that dichloroacetate accumulated on the TiO_2 powder surface is very persistent for further degradation both photocatalytically and thermally. It is likely that the active oxygen radicals important for initiating the photodegradation reactions appear to be unable to attack dichloroacetate residing

(63) Howe, R. F.; Gratzel, M. *J. Phys. Chem.* **1987**, *91*, 3906.
(64) Tanaka, K.-I. *J. Phys. Chem.* **1974**, *78*, 555.
(65) Shiotani, M.; Moro, G.; Freed, J. H. *J. Chem. Phys.* **1981**, *74*, 2616.
(66) d'Hennezel, O.; Ollis, D. F. In *11th International Congress on Catalysis. −40th Anniversary*; Hightower, J. W., Delgass, W. N., Iglesia, E., Bell, A. T., Eds. *Stud. Surf. Sci. and Catal.* **1996**, *101*, 435.

on the dark portions of the TiO_2 surface. Our experimental findings indicate that the diffusion of these active radical species is not great. Trichloracetate formation was not observed on the TiO_2 particle surface because the UV light was able to reach only a small minority of the TiO_2 surface, even though the evidence for trichloroacetate formation on Ti sites is strong (see section III.B.1). Hydration of the catalytic surface can serve to promote formation of acetic acids which are more mobile than the acetates and which can be photooxidized, although at a slow rate. Similar results have been observed by others using catalysts that were not as completely dehydrated as those in this study.[31,52]

IV. Conclusions

In situ SSNMR has been shown to be useful in investigating the photoinitiated surface reactions because of its ability to precisely identify reaction intermediates both in the gas phase and on the catalyst surface and to directly quantitate these species. Using these methods, the photocatalytic oxidation of TCE over titania-based catalysts has been studied. TCE degrades efficiently at the gas−solid interface in the presence of molecular oxygen to produce a number of long-lived intermediates. Oxygen radical species created via UV activation of added O_2 are likely candidates to be primarily involved in attacking the TCE double bond in the initiation step. The involvement of Cl radicals is an important feature in TCE photodegradation, whereas their role in the direct attack of the TCE double bond needs further investigation. DCAC and phosgene were major reaction intermediates identified in the TCE photooxidation reactions, and they were observed in all cases, both in TiO_2-based catalysts and in reactions over PVG. The formation of surface-bound dichloroacetate as a result of a surface reaction between mobile DCAC and surface hydoxyl groups was observed via ^{13}C CP/MAS experiments. Further destruction of dichloroacetate to phosgene and CO_2 was found to be slow but possible only in the presence of UV light and O_2, which indicates the advantage of employing TiO_2/PVG catalysts in reactors. However, once trichloroacetate was formed, it could not be effectively degraded, indicating that at least for surface adsorbates, hydrogen abstraction may play a key role in the degradation process.

Acknowledgment. Partial support for this research from the National Science Foundation (CHE 94-22235 and CHE 97-33188 CAREER Award), the Donors of the Petroleum Research Foundation administered by the American Chemical Society, and from the AT&T/Lucent Technologies Industrial Ecology Program is gratefully acknowledged. C.P. thanks the Purdue Research Foundation for a fellowship. D.R. is a Cottrell Scholar of the Research Corporation.

JA974192I